Journal of Cerebral Blood Flow & Metabolism (2011) 31, 2313–2323

www.jcbfm.com

Cortical substrate oxidation during hyperketonemia in the fasted anesthetized rat *in vivo*

Lihong Jiang[1], Graeme F Mason[1], Douglas L Rothman[1], Robin A de Graaf[1] and Kevin L Behar[2]

[1]*Department of Diagnostic Radiology, Magnetic Resonance Research Center, Yale University School of Medicine, The Anylan Center, New Haven, Connecticut, USA;* [2]*Department of Psychiatry, Magnetic Resonance Research Center, Yale University School of Medicine, The Anylan Center, New Haven, Connecticut, USA*

Ketone bodies are important alternate brain fuels, but their capacity to replace glucose and support neural function is unclear. In this study, the contributions of ketone bodies and glucose to cerebral cortical metabolism were measured *in vivo* in halothane-anesthetized rats fasted for 36 hours ($n=6$) and receiving intravenous [2,4-$^{13}C_2$]-D-β-hydroxybutyrate (BHB). Time courses of ^{13}C-enriched brain amino acids (glutamate-C4, glutamine-C4, and glutamate and glutamine-C3) were measured at 9.4 Tesla using spatially localized ^{1}H-[^{13}C]-nuclear magnetic resonance spectroscopy. Metabolic rates were estimated by fitting a constrained, two-compartment (neuron–astrocyte) metabolic model to the ^{13}C time-course data. We found that ketone body oxidation was substantial, accounting for 40% of total substrate oxidation (glucose plus ketone bodies) by neurons and astrocytes. D-β-Hydroxybutyrate was oxidized to a greater extent in neurons than in astrocytes ($\sim$70:30), and followed a pattern closely similar to the metabolism of [1-^{13}C]glucose reported in previous studies. Total neuronal tricarboxylic acid cycle (TCA) flux in hyperketonemic rats was similar to values reported for normal (nonketotic) anesthetized rats infused with [1-^{13}C]glucose, but neuronal glucose oxidation was 40% to 50% lower, indicating that ketone bodies had compensated for the reduction in glucose use.
Journal of Cerebral Blood Flow & Metabolism (2011) **31,** 2313–2323; doi:10.1038/jcbfm.2011.91; published online 6 July 2011

Keywords: energy metabolism; kinetic modeling; MR metabolite; MR spectroscopy; neuronal–glial interaction

Introduction

D-β-Hydroxylbutyrate (BHB), an end product of liver fatty acid catabolism, is actively used by the brain for energy metabolism, as well as for amino-acid and lipid biosynthesis. Under fasted conditions with declining blood glucose levels, ketone body levels increase from low levels of $\sim$0.1 to $\geqslant$3 mmol/L. During prolonged fasting or starvation, the brain's utilization of ketone bodies increase, primarily because of an increase in transport from the blood through monocarboxylic transporter proteins (Gjedde and Crone, 1975; Hasselbalch *et al*, 1996). Reports that ketone bodies are neuroprotective, including the well-known, but poorly understood, anticonvulsant effect of the ketogenic diet suggest that ketone bodies have actions beyond those of a simple fuel or synthetic substrate.

Although brain ketone oxidation can be substantial, the quantitative contribution of ketone bodies to neuronal and astroglial oxidative metabolism, and their capacity to replace glucose in support of neural function, remains unclear. In a study using [U-^{13}C]BHB, Kunnecke *et al* (1993) reported greater oxidation of ketone bodies in astrocytes than in neurons. Increased astroglial acetate metabolism has been observed in mice maintained on a ketogenic diet possibly reflecting adaptation to prolonged ketonemia (Melo *et al*, 2006; Yudkoff *et al*, 2005). In contrast, a study of acute hyperketonemia in overnight-fasted humans (Pan *et al*, 2001, 2002) infused intravenously with [2,4-$^{13}C_2$]-D-BHB revealed a pattern of brain glutamate and glutamine labeling similar to that from [1-^{13}C]glucose, indicating that oxidation of BHB, like glucose, occurred mostly in neurons—conclusions in line with results of early ^{14}C-labeled BHB tracer studies (Hawkins *et al*, 1986).

Correspondence: Dr L Jiang, TAC-MRRC, N147, PO Box 208043, New Haven, CT 06520, USA. E-mail: lihong.jiang@yale.edu or Dr KL Behar, TAC-MRRC, N151, PO Box 208043, New Haven, CT 06520, USA. E-mail: kevin.behar@yale.edu
This study was supported by NIH grants NIDDK R01-DK027121, NINDS P30-NS52519, and NIAAA K02 AA13430.
Received 4 February 2011; revised 7 May 2011; accepted 3 June 2011; published online 6 July 2011

Although brain utilization of ketone bodies is increased by fasting, contradictory findings have appeared on the effects of ketone bodies on brain glucose consumption. Early studies using [^{14}C] 2-deoxy-glucose (2-DG) autoradiography showed no effects on glucose uptake and oxygen consumption during acute infusion of BHB or after 3 days of fasting (Corddry *et al*, 1982), whereas later studies reported that ketone bodies administered acutely or increased over time by the ketogenic diet inhibited brain glucose utilization (LaManna *et al*, 2009; Melo *et al*, 2006).

In this study, we investigated the effects of hyperketonemia on cortical glucose and ketone metabolism of anesthetized rats subjected to a prolonged (36 hours) fast. Using [2,4-$^{13}C_2$]-D-BHB as a metabolic substrate administered by intravenous infusion, the turnover of ^{13}C-enriched glutamate and glutamine was measured *in vivo* using ^{1}H-nuclear magnetic resonance with indirect ^{13}C detection (^{1}H-[^{13}C] NMR). The ^{13}C-enrichment curves were fitted with a two-compartment metabolic model yielding the rates of BHB and glucose oxidation in neurons and astrocytes, and glutamate/glutamine neurotransmitter cycling.

Materials and methods

Animal Preparation

Experiments were conducted using male Sprague–Dawley rats (weighing 185 ± 15 g) fasted for 36 hours before study ($n = 6$). Rats were anesthetized with halothane (2% induction), tracheotomized, and ventilated (30% oxygen; ~68% nitrous oxide). After surgery, halothane was reduced to ~1% and D-tubocurarine-Cl was administered for immobilization. The left femoral artery and vein were catheterized for continuous monitoring of arterial blood pressure and blood sampling, and for infusion of [2.4-$^{13}C_2$]-D-BHB, respectively (Cambridge Isotopes, Andover, MA, USA). Blood gases (pCO_2, pO_2, pH) were measured periodically in arterial blood samples (ABL5 blood gas system, Radiometer America Inc., Westlake, OH, USA). Animal core body temperature was maintained near ~37°C using a heating pad connected to a temperature-regulated water bath.

Rats received [2,4-$^{13}C_2$]-D-BHB (1.5 mol/L) according to a three-step infusion: 0 to 5 minutes at 600 μmol/min per kg, 5 to 10 minutes at 300 μmol/min per kg, and thereafter at 120 μmol/min per kg. The three-step infusion protocol achieved a relatively rapid increase in plasma BHB with stable maintenance of blood BHB level and ^{13}C enrichment over the course of the ~90-minute infusion.

A separate small group ($n = 3$) of 36 hour-fasted rats was infused with [2-^{13}C]acetate (instead of ^{13}C-BHB) for 2 hours using a three-step infusion protocol (Jiang *et al*, 2009) and the brain tissue was studied *ex vivo.* Cerebral cortical extracts were prepared and ^{13}C metabolite enrichments determined to calculate the steady-state value of the flux ratio, V_{cyc}/V_{tcaN}, as described previously (Lebon *et al*, 2002; Patel *et al*, 2005), and subsequently used to constrain the fits of the metabolic model to the ^{13}C-enrichment time courses.

At the end of each animal experiment, the head and brain of the anesthetized animal were frozen *in situ* with liquid N_2 with continued mechanical ventilation.

All animal experiments were conducted under protocols approved by the Yale Animal Care and Use Committee.

In Vivo Nuclear Magnetic Resonance Spectroscopy

In vivo ^{1}H-[^{13}C] NMR spectra were obtained at 9.4 Tesla (Bruker ADVANCE NMR spectrometer/imager, Bruker BioSpin Corp., Billerica, MA, USA) (400.5 MHz for ^{1}H and 100.71 MHz for ^{13}C). The ^{13}C-edited ^{1}H NMR spectra were acquired using a circular surface coil of 14 mm diameter for ^{1}H detection, in which an outer butterfly coil was used for ^{13}C decoupling. Magnetic-field homogeneity was optimized using FASTMAP (Gruetter, 1993). The ^{1}H-[^{13}C] NMR spectra were obtained from a localized volume ($6 \times 6 \times 6\,mm^3$) using a polarization transfer pulse sequence in which the 90° and 180° pulses were replaced with adiabatic half- and full-passage pulses, respectively. Suppression of signals outside the localized volume was achieved with localization by adiabatic selective refocusing (de Graaf, 2007). The ^{1}H-[^{13}C] spectra were acquired with a 2.5-second repetition time in blocks of 512 scans with alternate on/off (180°) inversion of ^{13}C. Free induction decays were saved independently and processed in Matlab7.0 (MathWorks, Natick, MA, USA) for analyzing time-dependent changes. The time-dependent labeling of metabolites was analyzed by fitting the ^{1}H-[^{13}C] total and difference spectrum using an in-house written version of the linear-combination model algorithm implemented in Matlab (MathWorks). The concentrations of the metabolites were also determined in the brain extracts at the end point of the labeled isotope infusions.

Preparation of Blood Plasma and Brain Extracts and Nuclear Magnetic Resonance Spectroscopy

Plasma samples were prepared for NMR spectral analysis by the addition of 200 μL of 2.5 mmol/L formic acid and 0.25 mmol/L TSP (3-trimethylsilyl tetradeuterated sodium propionate) and 400 μL 100 mmol/L phosphate buffer (pH 7) to 50 μL blood plasma. The solution was passed through a microcentrifuge filter tube (10,000 Da cutoff, Nanosep Centrifugal Devices, VWR, Batavia, IL, USA). Concentrations and ^{13}C enrichments of BHB and other substances (such as acetoacetate, acetone, acetate, lactate) were determined using ^{1}H-[^{13}C] NMR spectroscopy with 20-second repetition time to achieve full spin-lattice T_1 relaxation of the measured metabolite resonances. Plasma and tissue extract samples were measured at 500 MHz (Bruker AVANCE high-resolution NMR spectrometer, Bruker BioSpin Corp., Billerica, MA, USA). Both TSP and formic acid were used as chemical shift and concentration references, respectively.

Ethanol extracts were prepared from the frozen fronto-parietal cortex (100 to 150 mg wet weight) using the procedure described in the study by Patel *et al* (2001). [2-^{13}C]glycine (50 μL, 5 mmol/L) was added as an internal concentration reference at the beginning of tissue extraction.

After centrifugation and lyophilization of the supernatant, the extract powder was suspended in 600 μL of a buffer solution containing 50 mmol/L phosphate (pH 7), 0.8 mmol/L formic acid, and 0.08 mmol/L TSP in D_2O/H_2O (2:1). The concentrations and ^{13}C enrichments of metabolite resonances in the extracted brain samples were measured fully relaxed (repetition time = 20 seconds) with ^{1}H-[^{13}C] NMR spectroscopy.

Description of the Metabolic Model Incorporating D-β-Hydroxybutyrate Oxidation

The time courses of brain amino-acid ^{13}C enrichments were fitted to a two-compartment metabolic model (Figure 1), using as input the plasma time courses of ^{13}C-enriched BHB, glucose, and lactate. In addition, nonlabeled sources (set to natural abundance) were included in the model to represent dilution flows. The metabolic model was fitted to the time courses of Glu-C4, Gln-C4, and Glx-C3 enrichment, along with the end-point enrichments for Gln-C3 and Glu-C3 (determined in the extracts). The differential equations describing the model (mass and isotope balance) were generated using CWave software (GF Mason, New Haven, CT, USA; Mason *et al*, 2003) and are given in Table 1. The differential equations were solved in Matlab using a first/second-order Runge–Kutta algorithm, and data were fitted using the Levenburg–Marquardt algorithm. Tissue glutamine was assumed to be present entirely in astrocytes, whereas glutamate was divided between neurons (90%) and astrocytes (10%) (Patel *et al*, 2005; Storm-Mathisen *et al*, 1983). Pyruvate carboxylase flux (V_{pc}) was assumed to be 20% of the rate of glutamine synthesis (V_{gln}) (Sibson *et al*, 2001). To improve the reliability of flux estimates, the fits were constrained by the value of the ratio, V_{cyc}/V_{tcaN} (Patel *et al*, 2005). The flux ratio was calculated from steady-state Glu-C4 and Gln-C4 ^{13}C enrichments (fe_{ss}) measured in a separate group of 36 hour-fasted animals receiving an infusion of [2-^{13}C]acetate according to:

$$V_{cyc}/V_{tcaN} = (fe_{ss}\text{Glu-C4}_N - c)/(fe_{ss}\text{Gln-C4} - fe_{ss}\text{Glu-C4}_N)$$

where 'c' is a correction to remove label incorporation arising from ^{13}C-labeled plasma glucose (C1,6), lactate (C3), and BHB (C2,4) by peripheral metabolism of the [2-^{13}C]acetate. The contribution of ^{13}C-labeled plasma glucose and/or lactate to Glu-C4 was determined from the steady-state enrichment of brain lactate C3 (fe_{ss}Lac-C3), which was assumed to be equivalent to the enrichment of pyruvate-C3, multiplied by the fraction of acetyl-CoA ^{13}C labeling derived through pyruvate and pyruvate dehydrogenase and given by

$$fe_{ss}\text{Glu-C4}_{pdh} = fe_{ss}\text{Lac-C3}_{Ac} \times (V_{pdhN}/V_{tcaN})$$

The contribution to Glu C4 enrichment from ketone bodies (BHB) is given by

$$fe_{ss}\text{Glu-C4}_{kb} = fe_{ss}\text{BHB-C4}_{Ac} \times (V_{AcCoA\text{-}kbN}/V_{tcaN})$$

Assuming that the neuronal acetyl-CoA pool is derived only from pyruvate and BHB, the value of 'c' can be expressed as:

$$c = fe_{ss}\text{Lac-C3}_{Ac} \times (1 - V_{AcCoA\text{-}kbN}/V_{tcaN}) - fe_{ss}\text{BHB-C4}_{Ac} \times V_{AcCoA\text{-}kbN}/V_{tcaN}$$

where the value for $V_{AcCoA\text{-}kbN}/V_{tcaN}$ was estimated from BHB-infused fasted animals and scaled downward proportionally to reflect the lower plasma BHB levels (3.8 ± 0.2 mmol/L, ^{13}C enrichment 16% ± 5%) in fasted [2-^{13}C]acetate-infused animals.

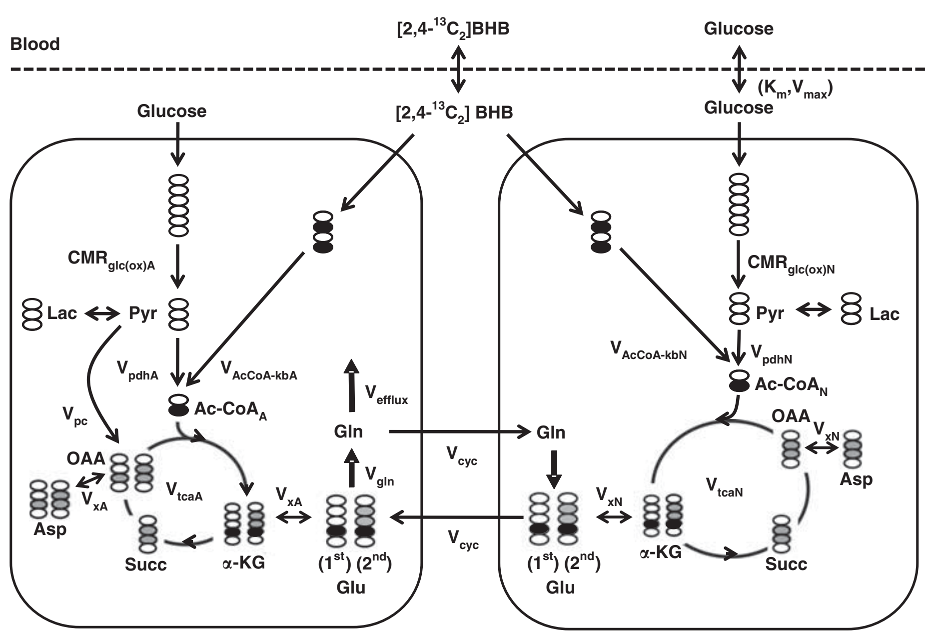

Figure 1 Two-compartment (neuron and astrocyte) model used to illustrate the metabolic pathway of label flow from BHB. $CMR_{kb} = (V_{AcCoA-kbA} + V_{AcCoA-kbN})/2$, $CMR_{glc(ox)} = (V_{pdhA} + V_{pdhN} + V_{pc})/2$. The OAA label distribution in astrocytes is shown for the pathway from succinate (equal labeling of OAA at C2 and C3) and pyruvate carboxylase (unlabeled carbon entry and dilution of OAA at C2). BHB, D-β-hydroxybutyrate; OAA, oxaloacetate.

Table 1 Differential equations describing the two-compartment model

Mass balance equations	
$dL/dt = 2CMR_{glc(ox)} - [V_{pc} + V_{pdhA} + V_{pdhN}]$	L, brain lactate
$dnGlu/dt = V_{cyc} + V_{xN(KGGlu)} - [V_{cyc} + V_{xN(GluKG)}]$	nGlu: neuronal glutamate, 90% of total glutamate
$daGlu/dt = V_{cyc} + V_{xA(KGGlu)} - [V_{gln} + V_{xA(GluKG)}]$	aGlu: astrocytic glutamate, 10% of total glutamate
$dGln/dt = V_{gln} - [V_{efflux} + V_{cyc}]$	Gln: glutamine concentration, only in astrocytes
$daKG/dt = V_{pdhA} + V_{xA(GluKG)} + V_{AcCoA\text{-}kbA} - [V_{tcaANet} + V_{xA(KGGlu)}]$	aKG: astrocytic α-ketoglutarate
$dnKG/dt = V_{xN(GluKG)} + V_{pdhN} + V_{AcCoA\text{-}kbN} - [V_{xN(KGGlu)} + V_{tcaN}]$	nKG: neuronal α-ketoglutarate
$daOAA/dt = 0.5V_{tcaANet} + 0.5V_{tcaANet} + V_{pc} - V_{tcaA}$	aOAA: astrocytic oxaloacetate
$dnOAA/dt = V_{xNAspOAA} + V_{tcaN} - [nV_{xNOAAAsp} + V_{tcaN}]$	nOAA: neuronal oxaloacetate
$nAsp/dt = V_{xN(OAAAsp)} - V_{xN(AspOAA)}$	nAsp: neuronal aspartate
$aAsp/dt = V_{xA(OAAAsp)} - V_{xA(AspOAA)}$	aAsp: astrocytic aspartate
Isotope balance equations	
$dL_3/dt = CMR_{glc(ox)}(Brain\_Glucose_{1,6}/Brain\_Glucose) + V_{dilLac}(Lac_3/Lac) - [V_{pc} + V_{dilLac} + V_{pdhA} + V_{pdhN}](L_3/L)$	
$daKG_4/dt = V_{pdhA}(L_3/L) + V_{xA(GluKG)}(aGlu_4/aGlu) + V_{AcCoA\text{-}kbA}(Brain\_BHB_{2,4}/Brain\_BHB) + V_{dilA}(Nat\_Abund_0/Nat\_Abund) - [V_{tcaANet} + V_{xA(KGGlu)}](aKG_4/aKG)$	
$daKG_3/dt = V_{xA(GluKG)}(aGlu_3/aGlu) + V_{tcaA}(aOAA_3/aOAA) - [V_{tcaANet} + V_{xA(KGGlu)}](aKG_3/aKG)$	
$dnKG_4/dt = V_{xN(GluKG)}(nGlu_4/nGlu) + V_{pdhN}(L_3/L) + V_{AcCoA\text{-}kbN}(Brain\_BHB_{2,4}/Brain\_BHB) - [V_{xN(KGGlu)} + V_{tcaN}](nKG_4/nKG)$	
$dnKG_3/dt = V_{xN(GluKG)}(nGlu_3/nGlu) + V_{tcaN}(nOAA_3/nOAA) - [V_{xN(KGGlu)} + V_{tcaN}](nKG_3/nKG)$	
$daGlu_3/dt = V_{xA(KGGlu)}(aKG_3/aKG) + V_{cyc}(nGlu_3/nGlu) - [V_{gln} + V_{xA(GluKG)}](aGlu_3/aGlu)$	
$dGln_3/dt = V_{gln}(aGlu_3/aGlu) - [V_{efflux} + V_{cyc}](Gln_3/Gln)$	
$daGlu_4/dt = V_{cyc}(nGlu_4/nGlu) + V_{xA(KGGlu)}(aKG_4/aKG) - [V_{gln} + V_{xA(GluKG)}](aGlu_4/aGlu)$	
$dnGlu_4/dt = V_{cyc}(Gln_4/Gln) + V_{xN(KGGlu)}(nKG_4/nKG) - [V_{cyc} + V_{xN(GluKG)}](nGlu_4/nGlu)$	
$dGln_4/dt = V_{gln}(aGlu_4/aGlu) - [V_{efflux} + V_{cyc}](Gln_4/Gln)$	
$dnGlu_3/dt = V_{cyc}(Gln_3/Gln) + V_{xN(KGGlu)}(nKG_3/nKG) - [V_{cyc} + V_{xN(GluKG)}](nGlu_3/nGlu)$	
$dnOAA_3/dt = V_{xN(AspOAA)}(nAsp_3/nAsp) + 0.5V_{tcaN}(nKG_4/nKG) + 0.5V_{tcaN}(nKG_3/nKG) - [V_{xN(OAAAsp)} + V_{tcaN}](nOAA_3/nOAA)$	
$daOAA_3/dt = 0.5V_{tcaANet}(aKG_4/aKG) + 0.5V_{tcaANet}(aKG_3/aKG) + V_{xA(AspOAA)}(aAsp_3/aAsp) + 0.5V_{pc}(L_3/L) - [V_{xA(OAAAsp)} + V_{tcaA}](aOAA_3/aOAA)$	
$dnOAA_3/dt = V_{xN(AspOAA)}(nAsp_3/nAsp) + 0.5V_{tcaN}(nKG_4/nKG) + 0.5V_{tcaN}(nKG_3/nKG) - [V_{xN(OAAAsp)} + V_{tcaN}](nOAA_3/nOAA)$	
$daOAA_3/dt = 0.5V_{tcaANet}(aKG_4/aKG) + 0.5V_{tcaANet}(aKG_3/aKG) + V_{xA(AspOAA)}(aAsp_3/aAsp) + 0.5V_{pc}(L_3/L) - [V_{xA(OAAAsp)} + V_{tcaA}](aOAA_3/aOAA)$	
Combination pools	
GluTot4 = aGlu+nGlu; GluTot3 = aGlu+nGlu	Total glutamate concentration at C4; aGlu is set to 10% total Glu concentration, nGlu is set to 90% total Glu concentration. Total glutamate concentration at C3
Glx3 = Gln+aGlu+nGlu	Sum of glutamate and glutamine at C3
Rates	
$CMR_{glc(ox)} = (V_{pdhA} + V_{pdhN} + V_{pc})/2$	Cerebral metabolic rate of glucose oxidation
$V_{cyc} = 0.54 * V_{tcaN}$	Glutamate/glutamine cycling rate
$V_d = 0.77$ mL/g	Distribution space for glucose and BHB (assumed to be equivalent)
$V_{efflux} = V_{pc}$	Glutamine efflux rate balanced to pyruvate carboxylase flux
$V_{gln} = V_{cyc} + V_{efflux}$	Glutamine synthesis rate
V_{pdhA}	Astrocytic pyruvate dehydrogenase rate
V_{pdhN}	Neuronal pyruvate dehydrogenase
$V_{tcaA} = V_{pdhA} + V_{AcCoA\text{-}kbA}$	Astroglial TCA cycle rate
$V_{tcaN} = V_{pdhN} + V_{AcCoA\text{-}kbN}$	Neuronal TCA cycle rate
$V_{xA(GluKG)} = 5\ \mu$mol/min per g	Rate of flow from glial Glu to glial KG
$V_{xA(KGGlu)} = V_{xA(GluKG)} + V_{pc}$	Rate of flow from glial KG to glial Glu
$V_{xN(GluKG)} = V_{xN(KGGlu)} = 5\ \mu$mol/min per g	Rate of flow between neuronal KG and neuronal Glu
$V_{xA(AspOAA)} = V_{xA(OAAAsp)} = 5\ \mu$mol/min per g	Rates of flow between glial aspartate and glial OAA
$V_{xNAspOAA} = V_{xNOAAAsp} = 5\ \mu$mol/min per g	Rates of flow between neuronal aspartate and neuronal OAA

BHB, D-β-hydroxybutyrate; KB, ketone body.

Statistics

Metabolites concentrations, enrichments, and metabolic fluxes were reported as group average ± s.d. Monte Carlo analysis of each animal's data set was performed using CWave to assess the distribution of uncertainties in the model parameters for individual animals. The uncertainties in Monte Carlo fitting were smaller than the group variability for each parameter reported in this study, indicating that uncertainties were dominated by inter animal variation.

Results

Effects of Acute [2,4-$^{13}C_2$]-D-β-Hydroxybutyrate Infusion on Blood and Brain Ketone Bodies

Table 2 presents the concentrations and enrichments of blood ketone bodies before and during ^{13}C-BHB infusion. The preinfusion plasma BHB concentration was 3 ± 1 mmol/L, which was quickly increased to 6.5 ± 1 mmol/L giving an average enrichment of 66% ± 17% (Figure 2). The BHB infusions led to a small elevation in arterial blood pH (~0.15 Units) compared with the preinfusion baseline.

Blood levels of other ketone bodies were also increased and enriched with ^{13}C during ^{13}C-BHB infusion. Acetoacetate comprised ~40% to 44% of the plasma BHB level (Table 2) and was similarly enriched, but was not detected in brain spectra *in vivo* or in the extract, likely because of both low brain concentration and overlap with GABA-C2. Plasma levels of acetone increased ~3-fold during ^{13}C-BHB infusion and were highly enriched with ^{13}C (~40%). Acetone was observed in plasma and brain spectra *in vivo*, but not in brain extracts because of its high volatility and loss during lyophilization. Plasma acetate levels increased similarly to BHB and acetoacetate (2.1-fold) during ^{13}C-BHB infusion, although ^{13}C enrichment remained relatively low (1.6%, Table 2), indicating limited conversion of the infused ^{13}C-BHB to free acetate.

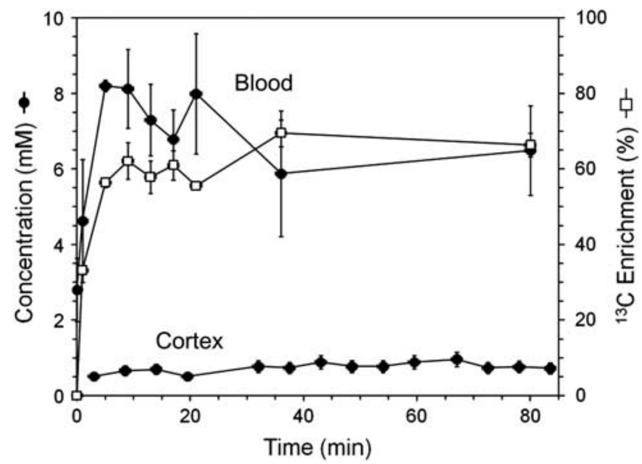

Figure 2 Time courses of BHB concentrations in the plasma and brain and ^{13}C enrichment (plasma). BHB, D-β-hydroxybutyrate.

Table 2 Concentrations and ^{13}C enrichments of substrates and metabolites in the plasma and cortical extracts from fasted rats at baseline (plasma) and after [2,4-$^{13}C_2$]-D-BHB infusion (plasma and brain)

	Baseline	*After BHB infusion (end point)*	
	Concentration (mmol/L)	*Concentration (mmol/L)*	*^{13}C enrichment (%)*
Blood plasma			
BHB	3.0 ± 1.0	6.5 ± 1.0	66 ± 17
AcAc	1.2 ± 0.6	2.9 ± 1.6	58 ± 4
Acetone	0.20 ± 0.08	0.6 ± 0.2	40 ± 4
Acetate	0.14 ± 0.02	0.3 ± 0.2	1.6 ± 0.8
Glucose	5.5 ± 1.8	6.9 ± 2.4	5.8 ± 2.2
Lactate	0.9 ± 0.3	2.7 ± 0.3	5.2 ± 2.2
Cerebral cortex			
BHB	0.26, 0.56[a]	0.7 ± 0.3	64 ± 7 (C4)
Acetone[b]	NA	0.025 ± 0.004	39 ± 4 (C1,3)
Glucose	0.96, 1.81[a]	2.7 ± 0.6	3.7 ± 0.2 (C1,6)
Lactate	1.7, 1.6[a]	2.8 ± 0.5	4.5 ± 1.1 (C3)
Alanine	0.47, 0.55[a]	0.8 ± 0.2	6.1 ± 1.7 (C3)
Aspartate	3.5, 2.8[a]	3.2 ± 0.8	14.9 ± 2.7 (C3)
Glutamate	12.4, 11.7[a]	11.9 ± 0.3	20.2 ± 3.3 (C3) 30.6 ± 2.9 (C4)
Glutamine	6.65, 6.58[a]	7.9 ± 1.2	16.7 ± 4.2 (C3) 25.0 ± 2.5 (C4)
GABA	1.35, 1.44[a]	1.4 ± 0.5	11.9 ± 2.2 (C2) 6.90 ± 2.2 (C3)

BHB, D-β-hydroxybutyrate; LC, linear combination; NA, not available.

[a]Cortical metabolite levels measured in extracts from two halothane-anesthetized animals fasted for 36 hours and prepared similarly but not infused with BHB. In these rats, the average concentration of plasma BHB was 3.9 mmol/L and that of lactate was 0.61 mmol/L. All other values represent mean ± s.d. Enrichment (%) reflects ^{13}C excess percentage enrichment above the natural abundance of 1.1%. All metabolites, except acetone, were measured in the end-point extract.

[b]Acetone concentration was determined from the LC model fitted *in vivo* spectrum.

Enrichment of Brain Amino Acids From [2,4-$^{13}C_2$]-D-β-Hydroxybutyrate

D-β-Hydroxybutyrate-C4 was readily detected in the brain ^{1}H-[^{13}C] difference spectra *in vivo* within the first 5 minutes of ^{13}C-BHB infusion (Figure 3A). Extensive incorporation of the ^{13}C label into the major brain amino-acid pools was seen (Figures 3A and 3B), appearing initially in glutamate (Glu)-C4, followed by glutamine (Gln)-C4, glutamate and glutamine (Glx)-C3, Glx-C2, and aspartate (Asp)-C3. Comparing the ^{1}H-[^{13}C] difference spectrum acquired at 96 minutes (Figure 3B) with the spectrum representing the sum of ^{12}C and ^{13}C (Figure 3C) shows the high enrichment of glutamate and glutamine from ^{13}C-BHB. The dynamic enrichment pattern is nearly identical to that observed when [1-^{13}C]glucose is the infused substrate (e.g., see the study by Pan *et al* (2002)). In addition to the enriched amino acids, ^{13}C-labeled acetone was also observed during ^{13}C-BHB infusion (Figure 3B; Supplementary Figure S1A), a product not observed during infusions of other substrates, such as [1,6-$^{13}C_2$]glucose or [2-^{13}C]acetate (Supplementary Figure S1B and C).

Table 2 depicts the total concentrations and end-point ^{13}C enrichments of cortical amino acids measured after 100 minutes of infusion of [2,4-$^{13}C_2$]-D-BHB. Inspection of the average end-point enrichments for Glu-C4 (30.6%), Gln-C4 (25%), and Asp-C3 (15%) shows values that are similar to those obtained from [1,6-^{13}C]glucose or [U-^{13}C]glucose for comparable plasma enrichment; however, GABA-C2 (11.9%) was much less. The steady-state GABA-C2/Glu-C4 ratio was only 0.40, which is considerably lower than that observed from ^{13}C-labeled glucose infused under the same anesthetic condition (halothane) (0.74, Chowdhury *et al*, 2007; 0.83, van Eijsden *et al*, 2010). As GABA levels (1.4 μmol/g) are similar to cortical levels determined in ^{13}C-glucose-infused, halothane-anesthetized rats (1.2 μmol/g, van Eijsden *et al*, 2010), the lower ^{13}C enrichment in GABA-C2 from ^{13}C-BHB in this study can be ascribed to a greater contribution of glucose (unlabeled dilution) to oxidative metabolism in GABA neurons.

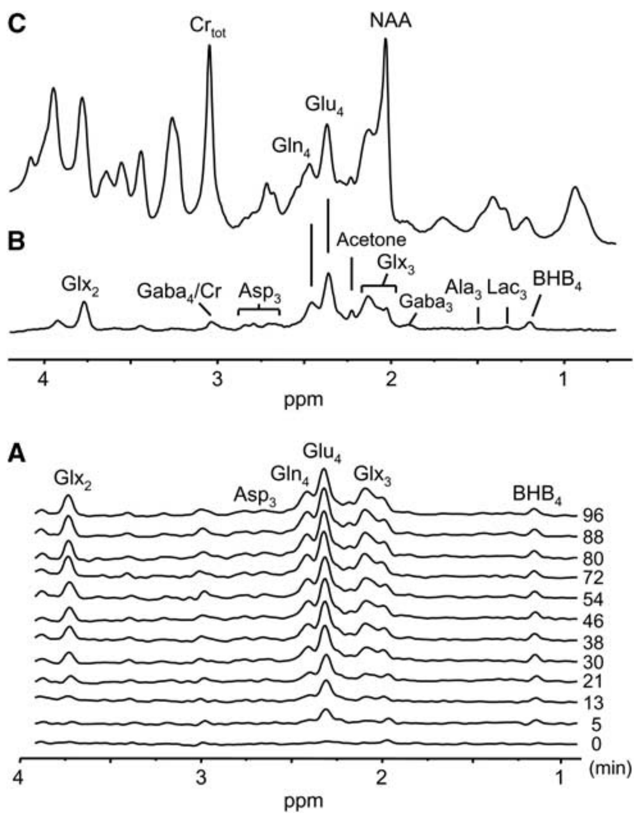

Figure 3 Spatially localized *in vivo* ^{1}H-[^{13}C] spectra of the rat cerebrum acquired during an intravenous infusion of [2,4-$^{13}C_2$]-D-BHB. (**A**) Time course of ^{1}H-[^{13}C] difference spectra acquired serially showing ^{13}C labeling of brain amino acids during the [2,4-$^{13}C_2$]-D-BHB infusion. The time of spectrum acquisition (midpoint, in minutes) is shown on the right. (**B**) ^{1}H-[^{13}C] difference spectrum reflecting ^{1}H atoms bound to ^{13}C atoms obtained by the difference of two acquired spectra with and without a ^{13}C inversion pulse as described in the 'Materials and methods' section. (**C**) ^{1}H-[^{13}C] spectrum of the sum of ^{12}C and ^{13}C resonances (total intensity). Carbonyl carbons are not detected in the ^{1}H-[^{13}C] difference spectra because of the absence of covalently bonded protons. BHB infusion begins at $t = 0$. Acquisition parameters: relaxation delay, 2.5 seconds; number of scans, 256; number of data points, 1,024, spectral volume, $6 \times 6 \times 6$ mm^3. Definitions: Cr$_{tot}$, total creatine; NAA, *N*-acetylaspartate; Glu, glutamate; Glx, glutamate + glutamine; Ala, alanine; Lac, lactate. BHB, D-β-hydroxybutyrate.

Assessment of Metabolic Fluxes

Figure 4 depicts time courses of cortical ^{13}C enrichments of Glu-C4 and Gln-C4 for a typical animal during [2,4-$^{13}C_2$]-D-BHB infusion. The solid lines reflect the best fits of the constrained two-compartment (neuron–astrocyte) metabolic model (Figure 1 and Table 1) to the time courses, which yielded the absolute rate estimates of ketone body and glucose

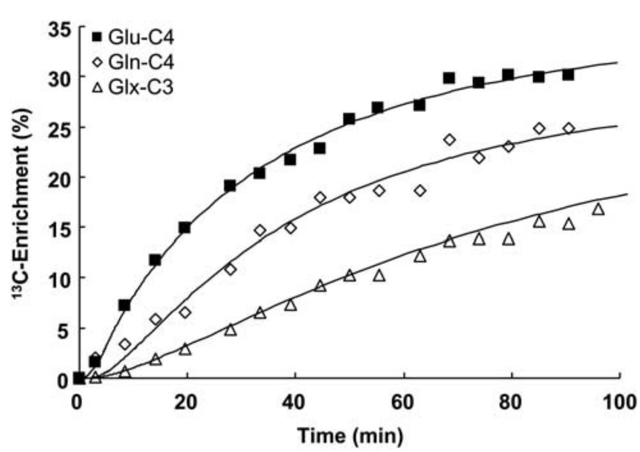

Figure 4 Time courses of ^{13}C enrichments of Gln-C4, Glu-C4, and Glx3, and best fits of the metabolic model for a 36 hour-fasted rat during [2,4-$^{13}C_2$]-BHB infusion. The brain amino-acid ^{13}C enrichments reflect the measured values (not normalized by plasma BHB ^{13}C enrichment). The average blood BHB ^{13}C enrichment was 65% for this animal. BHB, D-β-hydroxybutyrate.

Table 3 Estimates of cerebral metabolic fluxes (μmol/g per min) during hyperketonemia and [2,4-$^{13}C_2$]-D-BHB infusion determined by a constrained two-compartment (neuron–astrocyte) metabolic model

	$CMR_{glc(ox)}$	CMR_{kb}	$V_{AcCoA\text{-}kbN}$	$V_{AcCoA\text{-}kbA}$	V_{pdhA}	V_{pdhN}	V_{tcaN}	V_{tcaA}	V_{Gln}	V_{cyc}
Mean	0.33	0.22	0.31	0.14	0.29	0.29	0.60	0.42	0.40	0.32
Group s.d.	(0.13)	(0.04)	(0.16)	(0.09)	0.08	0.18	(0.32)	(0.13)	(0.21)	(0.17)
MCSD	(0.03)	(0.01)	(0.02)	(0.02)	0.04	0.03	(0.05)	(0.05)	(0.03)	(0.02)

BHB, D-β-hydroxybutyrate; MCSD, Monte-Carlo Standard Deviation.
Fluxes are given in units of μmol/g per min. Values represent mean ± s.d. of six animals. The metabolic model was fitted to the time courses for each animal individually and the parameter estimates (best fits) were averaged to give the values shown. V_{cyc}/V_{tcaN} was constrained to the value of the ratio (0.54) calculated from Glu-C4 and Gln-C4 enrichments measured at isotopic steady-state during an infusion of [2-^{13}C]acetate for a separate group of 36 hour-fasted rats (see the 'Materials and methods' section). V_{pc} was constrained to $0.2 \times V_{gln}$ (Sibson *et al*, 2001). MCSD is the mean s.d. from the 20-step Monte Carlo analysis of 6 animals, providing a measure of the quality of individual fits.

oxidation in neurons and astrocytes. The metabolic rates are summarized in Table 3. D-β-Hydroxybutyrate oxidation accounted for a substantial fraction (40% ± 5%) of the overall substrate oxidation of neurons and astrocytes. D-β-Hydroxybutyrate was oxidized quantitatively to a greater extent in neurons, however, accounting for ~70% of total ketone body consumption (neurons, 0.31 ± 0.16 μmol/g per min; astrocytes, 0.14 ± 0.09 μmol/g per min). Within the two different neural cell types, BHB contributed a slightly larger fraction of the total substrate oxidation in neurons (neurons, ~52%; astrocytes, ~33%).

The measured neuronal TCA cycle rate in 36 hour-fasted rats is similar to that seen in overnight-fasted, halothane-anesthetized rats infused with [1,6-^{13}C] or [U-^{13}C]glucose (0.47 to 0.55 μmol/g per min, van Eijsden *et al*, 2010; Jiang *et al*, 2009; Patel *et al*, 2004). In the latter studies, glucose accounts for >90% of oxidized substrate, such that $V_{pdhN} \approx V_{tcaN}$. In contrast to glucose-infused rats, V_{pdhN} (0.29 μmol/g per min) was ~40% to 50% lower in hyperketonemic rats indicating that BHB oxidation is compensated by an equal reduction in oxidation of glucose-derived acetyl-CoA.

Effects of Parameter Constraints on the Calculated Fluxes

The reliability of the estimated value of the glutamate/glutamine cycling flux (V_{cyc}) when iterated as a free parameter depends on the difference in the time courses of Glu-C4 and Gln-C4 (Shen *et al*, 2009). In contrast to the well-separated Glu-C4 and Gln-C4 enrichment curves seen in anesthetized rats infused with [1-^{13}C]glucose (Patel *et al*, 2005), the enrichment curves were closer together in [2,4-^{13}C]BHB-infused rats, decreasing reliability in the value of V_{cyc} as an iterated parameter. To improve reliability in flux estimates, the model fits were constrained by the ratio, V_{cyc}/V_{tcaN}, determined in 36 hour-fasted rats infused with the astroglial substrate, [2-^{13}C]acetate (see the 'Materials and methods' section) (Supplementary material, Table S1).

Fitting the metabolic fluxes with the V_{cyc}/V_{tcaN} ratio constrained (0.54) compared with V_{cyc} freely iterated improved the individual fits, reducing %MCSD (% Monte Carlo Standard Deviation) of V_{cyc} ~40% without significantly altering variance in V_{tcaN} and $V_{AcCoA\text{-}kb}$, effects consistent with previous analysis (Shen *et al*, 2009).

[2,4-^{13}C]BHB labels the TCA cycle and associated amino acids through [2-^{13}C]acetyl-CoA, and is relatively insensitive to glial anaplerosis (pyruvate carboxylase flux). Therefore, V_{pc} was constrained to a value equal to $0.2 \times V_{gln}$ based on a previous study of anesthetized rats infused with [2-^{13}C]glucose (Sibson *et al*, 2001). To assess the sensitivity of the calculated fluxes on the value of this parameter, a sensitivity analysis was performed by fitting the metabolic model to the ^{13}C time courses using different V_{pc}/V_{gln} ratio values, 50% below and 50% above the assumed value (Supplementary Material, Table S2). The analysis estimates the potential error in the calculated fluxes from their nominal values should the true value of the parameter be lower or higher than assumed. Relatively small differences from the nominal values were seen for lower values ($V_{pc}/V_{gln} = 0.1$, −3% to −10%), but differences became larger for higher values ($V_{pc}/V_{gln} = 0.3$, −44% to +35%), whereas fit quality was poor.

Discussion

In this study, we measured the contributions of ketone bodies and glucose to neuronal and astroglial oxidation in anesthetized rats made hyperketonemic by prolonged (36 hours) fasting and infused acutely with [2,4-^{13}C]-BHB. The following main conclusions can be drawn: (1) BHB oxidation in the fasted anesthetized rat cortex is extensive, accounting for ~40% of total TCA cycle flux; (2) quantitatively, BHB oxidation is greater in neurons (70% of total ketone consumption) than in astrocytes; and (3) comparisons with glucose-infused rats from previous studies show that ketone body oxidation is compensated by an equal reduction in glucose oxidation.

Comparison of Present Results With Previous Studies

Prolonged fasting is well known to enhance ketone body transport (Gjedde and Crone, 1975; Hasselbalch *et al*, 1996). The prolonged fast effectively produced a stable steady state of hyperketonemia before ^{13}C-labeled BHB infusion, thus avoiding the major brain metabolic/regulatory shifts in transitioning between glucose- and BHB-fed conditions. The brain-to-blood plasma ratio for BHB in 36 hour-fasted rats of 0.11 ± 0.04 agrees well with values from 48 hour-fasted rats (0.12, Hawkins *et al* (1971)), and is higher than that seen in fed rats infused acutely with ketone bodies (0.075, Hawkins *et al* (1971)), consistent with a fasting-induced enhancement in ketone body transport.

The rate of cortical ketone body oxidation, CMR_{kb} ($=1/2V_{AcCoA\text{-}kb}$) of $0.22 \pm 0.04\,\mu$mol/g per min, can be compared with previous estimates based on cerebral arteriovenous difference or ^{14}C-autoradiography. Assuming a net extraction ratio for BHB of $\sim$0.04 to 0.07 (Hawkins *et al*, 1971; Daniel *et al*, 1971; Gjedde and Crone, 1975; Conn *et al*, 1983) and for acetoacetate of $\sim$0.1 (Hawkins *et al*, 1971), and a brain blood flow of $\sim$0.62 mL/g per min (Dahlquist and Persson, 1976), the corresponding rates per unit blood concentration (mmol/L) is given by the product of the extraction ratio and cerebral blood flow, yielding $\sim$0.02 to 0.04 and $\sim$0.06 μmol/g per min per mmol/L, respectively. For plasma BHB and acetoacetate concentrations of 6.5 and 2.9 mmol/L, respectively (Table 1), CMR_{kb} would be $\sim$0.30 to 0.43 μmol/g per min. This value likely represents an upper estimate because extraction is assumed to be unidirectional with ketone bodies metabolized immediately upon entry. However, brain concentration of BHB (after correction for an assumed 3% blood volume) is not zero but is substantial (0.51 mmol/L), suggesting that net extraction (metabolism) is less than the values used above. Using clearance data from the ^{14}C-autoradiography study of Hawkins *et al* (1986) for the parietal cortex of 2 day-starved unanesthetized rats, ketone body influx (μmol/g per min) can be computed from the BHB clearance rate (0.025 mL/g per min), the ratio of acetoacetate and BHB clearance (1.46), and the present concentrations of BHB (6.5 mmol/L) and acetoacetate (2.9 mmol/L), and is given by: $CMR_{kb} = CMR_{BHB} + CMR_{AcAc} = (0.025 \times 6.5) + (0.025 \times 1.46 \times 2.9) = 0.27$ (± 0.08) μmol/g per min. Considering the differences between methods, conditions (awake versus anesthetized), brain tissue represented in the measurements (whole brain versus cortex), and rat strains/gender (Wistar females and Long-Evans males versus Sprague–Dawley males), the Magnetic Resonance Spectroscopy (MRS)-derived value for ketone body consumption *in vivo* is in reasonably good agreement with other approaches.

β-Hydroxybutyrate Oxidation in Cortical Neurons and Astrocytes

Glutamate is concentrated primarily in neurons, whereas glutamine is produced and concentrated in astrocytes. [2,4-$^{13}C_2$]D-β-hydroxybutyrate enters the TCA cycle as acetyl-CoA at C2, labeling citrate-C4 followed by α-ketoglutarate at C4, which through mitochondrial/cytoplasmic exchange with glutamate enriches Glu-C4 in the large cytoplasmic pool. Glutamate labeled in neurons is released during synaptic activity, taken up by astrocytes, and metabolized to glutamine. Thus, the relative kinetics of Glu-C4 and Gln-C4 labeling during an infusion of a ^{13}C-labeled substrate which labels acetyl-CoA at C2 (e.g., [1,6-$^{13}C_2$]glucose or [2-^{13}C]-acetate) reflects the relative preference of neurons and astrocytes for that substrate. During [2,4-^{13}C]-D-BHB infusion, the ^{13}C enrichment of Glu-C4 exceeded Gln-C4 at all times. This is consistent with findings using tracer levels of [3-^{14}C]BHB in unanesthetized 48-hour-fasted and ketotic adult rats (Cremer, 1971) and in preweanling rats, which are normally ketotic (DeVivo *et al*, 1975), and interpreted as BHB oxidation in the large glutamate pool associated with neurons. A study of the occipital cortex of overnight-fasted, awake healthy human subjects using ^{13}C MRS with [2,4-^{13}C]-D-BHB infusion also shows the same labeling pattern, similar to that produced from [1-^{13}C]glucose, and attributed to neuronal oxidation (Pan *et al*, 2002).

However, our findings contrast with those of Kunnecke *et al* (1993) who reported a higher labeling ratio in brain Gln-C4 relative to Glu-C4 (Gln/Glu >1) during acute hyperketonemia in fed rats receiving infusions of [U-^{13}C]BHB, and was interpreted as a greater metabolism of ketone bodies in astrocytes than in neurons. It is not clear whether dietary status alone (fed versus fasted) might produce this effect. Enhanced glutamine synthesis has been reported in mice fed the ketogenic diet after intraperitoneal injection of [1,2-^{13}C]acetate and [1-^{13}C]glucose (Melo *et al*, 2006; Yudkoff *et al*, 2005), suggesting that astrocytes may adapt to prolonged ketosis, but this condition would have been anticipated in fasted rats rather than in fed rats. The influence of dietary status (fed, fasted, ketogenic diet) and species on astrocyte metabolism during hyperketonemia *in vivo* merits further study.

Effects of Hyperketonemia on Glucose Utilization in the Cerebral Cortex

The neuronal TCA cycle rate of hyperketonemic-fasted animals in our study ($0.60 \pm 0.32\,\mu$mol/min per g) is similar to our previously reported values from overnight-fasted, halothane-anesthetized rats infused with [1,6-^{13}C]glucose, as measured from a comparable brain region and spectroscopic volume (0.52 to 0.53 μmol/min per g (Patel *et al*, 2004; van Eijsden *et al*, 2010)). This observation is consistent with previous studies of rats showing that brain oxygen consumption (which is proportional to TCA cycle activity) is unaffected by hyperketonemia whether by acute BHB infusion (Linde *et al*, 2006) or by starvation for 48 to 72 hours (Dahlquist and Persson, 1976; Hawkins, 1971).

As total rates of substrate oxidation (TCA cycle flux) in neurons and astrocytes seemed similar to their respective values in nonketonemic, ^{13}C-glucose-infused, anesthetized rats (Patel *et al*, 2005), we conclude that BHB oxidation was compensated by an equivalent reduction in acetyl-CoA oxidation from glucose. Previous studies have reported inconsistent findings regarding the effects of hyperketonemia on glucose utilization. In an early study of brain slices/minces, Openshaw and Bortz (1968) reported that ketone body elevation decreased glucose oxidation, whereas others reported increased lactate formation with no change in glucose oxidation (Ito and Quastel, 1970; Rolleston and Newsholme, 1967). Studies reporting brain glucose utilization by arterio/venous difference (Linde *et al*, 2006) or ^{14}C-2-deoxyglucose phosphorylation (Corddry *et al*, 1982; Crane *et al*, 1985) in rats during hyperketonemia, whether induced by fasting (2 to 3 days) or by acute BHB infusion, consistently show no change in CMR_{glc} compared with the fed condition, unless fasting is more prolonged when a decrease in CMR_{glc} occurs (Crane *et al*, 1985). The findings that increased oxidation of ketone bodies occurs without altering either glucose or oxygen consumption suggest that glucose metabolism during hyperketonemia is diverted to lactate production and efflux to the blood, which may occur transiently, as reported by Hawkins *et al* (1971).

Brain lactate was elevated in end-point extracts when compared with rats fasted for a comparable time (36 hours) but not infused with BHB (Table 2), although animal numbers were too few at baseline for statistical assessment. As plasma lactate levels also increased during ^{13}C-BHB infusion, we cannot say whether the higher brain lactate reflects blood level changes, or possibly reduced intracellular clearance caused by the reduction in pyruvate/lactate oxidation and efflux as described by Pan *et al* (2000) in 2 to 3 day-fasted human subjects. As a cautionary note, extract measurements are susceptible to postmortem effects that can increase brain lactate, and whereas rats in our study were ventilated during brain freezing to reduce the likelihood of agonal change, this possibility cannot be excluded entirely.

Few *in vivo* studies are available that report glucose oxidation, as opposed to glucose uptake (arterio/venous difference) or phosphorylation (^{14}C-2-deoxyglucose autoradiography). One exception is the study by Mans *et al* (1987), who found a small decrease in glucose oxidation ($\sim$12% averaged over the whole brain) in unanesthetized rats fasted for 2 days compared with fed rats. These authors used quantitative autoradiography with short time infusion (5 minutes) of [6-^{14}C]glucose, which is metabolized and trapped mainly as ^{14}C-labeled amino acids, a technique most closely related to the NMR approach in this study. The larger reduction in glucose oxidation assessed in this study would be expected based on the much greater plasma BHB level (6.5 mmol/L) compared with the study by Mans *et al* (0.85 mmol/L).

Rodents subjected to prolonged hyperketonemia through a high-fat (ketogenic) diet show similar effects on glucose metabolism to those seen after short periods of fasting (< 3 days), in that glucose oxidation is reduced but glucose uptake (phosphorylation) is unaltered. al-Mudallal *et al* (1995) found no alteration in regional CMR_{glc} based on ^{14}C-2-deoxyglucose phosphorylation in rats fed a ketogenic diet for 6 to 7 weeks. In contrast, in mice fed a ketogenic diet for 2 weeks followed by injection of [1-^{13}C]glucose, significant reductions were reported in ^{13}C labeling of brain metabolites and amino acids (Yudkoff *et al*, 2005; Melo *et al*, 2006).

Interestingly, in contrast to findings in rodents, prolonged fasting or acute BHB infusion in humans is associated with reduced brain glucose utilization (26% to 33%) as measured by positron emission tomography with [^{18}F]2-fluoro-2-deoxy-D-glucose or arterio/venous difference methods (Hasselbalch *et al*, 1996).

Potential Impact of Other ^{13}C-Labeled Ketones and Nonketone Substrates on the Analysis

The ^{13}C enrichments of acetoacetate and acetone were not considered in the present analysis, although both were highly enriched (Table 2). Acetoacetate is an intermediate in BHB catabolism and is in fast equilibrium with BHB; hence, its time course of labeling would be expected to be proportional to BHB. As acetoacetate was not detected in the brain spectra, and the transport kinetics of acetoacetate across the blood–brain barrier is uncertain, the use of blood or brain acetoacetate levels as a driver was precluded. We also did not account for the labeled acetone in the metabolic model. As acetone is highly volatile, it is likely to be exhaled and may not contribute significantly as a fuel substrate. However, acetone can be metabolized by the liver and labels plasma glucose in fasted humans (Reichard *et al*, 1979) and in rats under normal and diabetic ketotic conditions, as well as BHB in ketosis (Kosugi *et al*, 1986).

Any labeling of BHB-C4,2 by acetone-C1,3 would not be distinguished from the infused ^{13}C-BHB used as the input.

Blood glucose ^{13}C enrichment (5.8% in C1) was detected in fasted/^{13}C-BHB-infused animals at $\sim$90 minutes, which would not be distinguished from the ^{13}C-BHB because both substrates lead to the same labeling pattern for acetyl-CoA. Although we cannot specifically address its origin, we included the labeled glucose as an additional driver (input) in the modeling (Table 1) by assuming that glucose enrichment increased linearly over the period of the ^{13}C-BHB infusion and that glucose-C1 and glucose-

C6 were equally enriched. Although acetyl-CoA derived from glucose represented ~56% of total acetyl-CoA (the rest supplied by ketone bodies), the low plasma glucose enrichment of 5.8% would be expected to result in a relatively small contribution ($0.56 \times 0.058 \times 100 = 3.2\%$) to the glutamate-C4 end-point enrichment at isotopic steady state.

Ketone Body Utilization in Relation to Aspartate and GABA

The steady-state labeling of aspartate (Asp) and GABA relative to glutamate or glutamine from [2,4-^{13}C]-D-BHB (Table 2) is much less than is seen for nonketonemic animals prepared similarly but infused with [1-^{13}C], [1,6-^{13}C], or [U-^{13}C]glucose (Tyson *et al*, 2003; van Eijsden *et al*, 2010). Values of the steady-state enrichment ratios of Asp-C3/Glu-C4 (0.49) and GABA-C2/Glu-C4 (0.39) were lower than respective values seen in glucose-infused rats (>0.75). This observation indicates that Asp and GABA do not share the same acetyl-CoA precursor pool with the large glutamate pool (glutamatergic neurons) in terms of relative flows of ketone bodies and glucose. DeVivo *et al* (1975) compared ^{14}C labeling of brain amino acids in brain's of developing rats from tracer doses of [2-^{14}C]glucose or [3-^{14}C]BHB, finding a lower GABA/Glu ^{14}C-specific activity ratio after postnatal day 15, and concluded that BHB was less effective than glucose as a substrate for GABA synthesis after this postnatal age. In our study, the similar percentage reductions in Asp and GABA labeling from [2,4-^{13}C]-D-BHB compared with [1,6-^{13}C]glucose, could be explained if Asp was more concentrated in GABAergic neurons than in astrocytes. Furthermore, because steady-state GABA labeling from ^{13}C-BHB appeared less than would be expected from ^{13}C-glucose, our results indicate that glucose is preferred over BHB as a fuel for GABAergic neurons. Reduced labeling of Asp was also reported in a ^{13}C MRS study of human subjects infused with [2,4-^{13}C]-D-BHB (Pan *et al*, 2002). Steady-state ^{13}C labeling of Asp (C3) relative to Glu (C4,C3) was much less than expected had Asp and Glu labeling from BHB occurred in the same cellular (neuronal) pool, suggesting that Asp was mostly present in nonglutamatergic cells, possibly astrocytes or GABAergic neurons. These findings concur, suggesting that Asp may be enriched in GABAergic neurons.

Conclusions

In summary, our results show that in anesthetized rats fasted for 36 hours, ketone bodies can support as much as 40% of total substrate oxidation in the cerebral cortex. Neurons and astrocytes oxidize BHB, although neurons consume the most and in a pattern similar to glucose. The oxidation of ketone bodies is compensated by reduced oxidation of glucose resulting in an apparently unaltered TCA cycle flux. Further experiments are required to define the range over which ketone body oxidation can be increased. This is important because of recent work indicating that transport and utilization of acetate (and possibly other monocarboxylic acids) is increased in humans with type 1 diabetes (Mason *et al*, 2006). The capacity of brain cells to oxidize substrates other than glucose (e.g., acetate, ketone bodies, free fatty acids, etc.) could provide significant therapeutic opportunities to enhance neuronal and astroglial function during times of hypoglycemic stress.

Acknowledgements

The authors thank Ms Bei Wang for assistance in animal preparation.

Disclosure/Conflict of interest

The authors declare no conflict of interest.

References

al-Mudallal AS, Levin BE, Lust WD, Harik SI (1995) Effects of unbalanced diets on cerebral glucose metabolism in the adult rat. *Neurology* 45:2261–5

Chowdhury GM, Gupta M, Gibson KM, Patel AB, Behar KL (2007) Altered cerebral glucose and acetate metabolism in succinic semialdehyde dehydrogenase-deficient mice: evidence for glial dysfunction and reduced glutamate/glutamine cycling. *J Neurochem* 103:2077–91

Conn AR, Fell DI, Steele RD (1983) Characterization of α-keto acid transport across blood-brain barrier in rats. *Am J Physiol* 245:E253–60

Corddry DH, Rapoport SI, London ED (1982) No effect of hyperketonemia on local cerebral glucose utilization in conscious rats. *J Neurochem* 38:1637–41

Crane PD, Pardridge WM, Braun LD, Oldendorf WH (1985) Two-day starvation does not alter the kinetics of blood–brain barrier transport and phosphorylation of glucose in rat brain. *J Cereb Blood Flow Metab* 5:40–6

Cremer JE (1971) Incorporation of label from D-β-hydroxy-(^{14}C)butyrate and (3-^{14}C)acetoacetate into amino acids in rat brain *in vivo*. *Biochem J* 122:135–8

Dahlquist G, Persson B (1976) The rate of cerebral utilization of glucose, ketone bodies, and oxygen: a comparative *in vivo* study of infant and adult rats. *Pediatr Res* 10:910–7

Daniel PM, Love ER, Moorehouse SR, Pratt OE, Wilson P (1971) Factors influencing utilisation of ketone-bodies by brain in normal rats and rats with ketoacidosis. *Lancet* 2:637–8

de Graaf RA (2007) *In Vivo NMR Spectroscopy/Principals and Techniques*. John Wiley&Sons, Ltd: Hoboken, NJ, USA

DeVivo DC, Malas KL, Leckie MP (1975) Starvation and seizures. Observation on the electroconvulsive threshold and cerebral metabolism of the starved adult rat. *Arch Neurol* 32:755–60

Gjedde A, Crone C (1975) Induction processes in blood-brain transfer of ketone bodies during starvation. *Am J Physiol* 229:1165–9
Gruetter R (1993) Automatic localized *in vivo* adjustment of all first- and second- order shim coils. *Magn Reson Med* 29:804–11
Hasselbalch SG, Madsen PL, Hageman LP, Olsen KS, Justesen N, Holm S, Paulson OB (1996) Changes in cerebral blood flow and carbohydrate metabolism during acute hyperketonemia. *Am J Physiol* 270: E746–51
Hawkins RA (1971) Uptake of ketone bodies by rat brain *in vivo*. *Biochem J* 121:17P
Hawkins RA, Mans AM, Davis DW (1986) Regional ketone body utilization by rat brain in starvation and diabetes. *Am J Physiol* 250:E169–78
Hawkins RA, Williamson DH, Krebs HA (1971) Ketone-body utilization by adult and suckling rat brain *in vivo*. *Biochem J* 122:13–8
Ito T, Quastel JH (1970) Acetoacetate metabolism in infant and adult rat brain *in vitro*. *Biochem J* 116: 641–55
Jiang L, Herzog RI, Mason GF, de Graaf RA, Rothman DL, Sherwin RS, Behar KL (2009) Recurrent antecedent hypoglycemia alters neuronal oxidative metabolism *in vivo*. *Diabetes* 58:1266–74
Kosugi K, Chandramouli V, Kumaran K, Schumann WC, Landau BR (1986) Determinants in the pathways followed by the carbons of acetone in their conversion to glucose. *J Biol Chem* 261:13179–81
Kunnecke B, Cerdan S, Seelig J (1993) Cerebral metabolism of [1,2-$^{13}C_2$]glucose and [U-$^{13}C_4$]3-hydroxybutyrate in rat brain as detected by ^{13}C NMR spectroscopy. *NMR Biomed* 6:264–77
LaManna JC, Salem N, Puchowicz M, Erokwu B, Koppaka S, Flask C, Lee Z (2009) Ketones suppress brain glucose consumption. *Adv Exp Med Biol* 645:301–6
Lebon V, Petersen KF, Cline GW, Shen J, Mason GF, Dufour S, Behar KL, Shulman GI, Rothman DL (2002) Astroglial contribution to brain energy metabolism in humans revealed by ^{13}C nuclear magnetic resonance spectroscopy: elucidation of the dominant pathway for neurotransmitter glutamate repletion and measurement of astrocytic oxidative metabolism. *J Neurosci* 22:1523–31
Linde R, Hasselbalch SG, Topp S, Paulson OB, Madsen PL (2006) Global cerebral blood flow and metabolism during acute hyperketonemia in the awake and anesthetized rat. *J Cereb Blood Flow Metab* 26:170–80
Mans AM, Davis DW, Hawkins RA (1987) Regional brain glucose use in unstressed rats after two days of starvation. *Metab Brain Dis* 2:213–21
Mason GF, Falk Petersen K, de Graaf RA, Kanamatsu T, Otsuki T, Shulman GI, Rothman DL (2003) A comparison of ^{13}C NMR measurements of the rates of glutamine synthesis and the tricarboxylic acid cycle during oral and intravenous administration of [1-^{13}C]glucose. *Brain Res Brain Res Protoc* 10:181–90
Mason GF, Petersen KF, Lebon V, Rothman DL, Shulman GI (2006) Increased brain monocarboxylic acid transport and utilization in type 1 diabetes. *Diabetes* 55:929–34
Melo TM, Nehlig A, Sonnewald U (2006) Neuronal-glial interactions in rats fed a ketogenic diet. *Neurochem Int* 48:498–507
Openshaw H, Bortz WM (1968) Oxidation of glucose, acetoacetate, and palmitate in brain mince of normal and ketotic rats. *Diabetes* 17:90–5
Pan JW, de Graaf RA, Petersen KF, Shulman GI, Hetherington HP, Rothman DL (2002) [2,4-^{13} C_2]-β-Hydroxybutyrate metabolism in human brain. *J Cereb Blood Flow Metab* 22:890–8
Pan JW, Rothman TL, Behar KL, Stein DT, Hetherington HP (2000) Human brain beta-hydroxybutyrate and lactate increase in fasting-induced ketosis. *J Cereb Blood Flow Metab* 20:1502–7
Pan JW, Telang FW, Lee JH, de Graaf RA, Rothman DL, Stein DT, Hetherington HP (2001) Measurement of β-hydroxybutyrate in acute hyperketonemia in human brain. *J Neurochem* 79:539–44
Patel AB, de Graaf RA, Mason GF, Kanamatsu T, Rothman DL, Shulman RG, Behar KL (2004) Glutamatergic neurotransmission and neuronal glucose oxidation are coupled during intense neuronal activation. *J Cereb Blood Flow Metab* 24:972–85
Patel AB, de Graaf RA, Mason GF, Rothman DL, Shulman RG, Behar KL (2005) The contribution of GABA to glutamate/glutamine cycling and energy metabolism in the rat cortex *in vivo*. *Proc Natl Acad Sci USA* 102:5588–93
Patel AB, Rothman DL, Cline GW, Behar KL (2001) Glutamine is the major precursor for GABA synthesis in rat neocortex *in vivo* following acute GABA-transaminase inhibition. *Brain Res* 919:207–20
Reichard Jr GA, Haff AC, Skutches CL, Paul P, Holroyde CP, Owen OE (1979) Plasma acetone metabolism in the fasting human. *J Clin Invest* 63:619–26
Rolleston FS, Newsholme EA (1967) Effects of fatty acids, ketone bodies, lactate and pyruvate on glucose utilization by guinea-pig cerebral cortex slices. *Biochem J* 104:519–23
Shen J, Rothman DL, Behar KL, Xu S (2009) Determination of the glutamate-glutamine cycling flux using two-compartment dynamic metabolic modeling is sensitive to astroglial dilution. *J Cereb Blood Flow Metab* 29: 108–18
Sibson NR, Mason GF, Shen J, Cline GW, Herskovits AZ, Wall JE, Behar KL, Rothman DL, Shulman RG (2001) *In vivo* ^{13}C NMR measurement of neurotransmitter glutamate cycling, anaplerosis and TCA cycle flux in rat brain during [2-^{13}C]glucose infusion. *J Neurochem* 76:975–89
Storm-Mathisen J, Leknes AK, Bore AT, Vaaland JL, Edminson P, Haug FM, Ottersen OP (1983) First visualization of glutamate and GABA in neurones by immunocytochemistry. *Nature* 301:517–20
Tyson RL, Gallagher C, Sutherland GR (2003) ^{13}C-labeled substrates and the cerebral metabolic compartmentalization of acetate and lactate. *Brain Res* 992:43–52
van Eijsden P, Behar KL, Mason GF, Braun KP, de Graaf RA (2010) *In vivo* neurochemical profiling of rat brain by ^{1}H-[^{13}C] NMR spectroscopy: cerebral energetics and glutamatergic/GABAergic neurotransmission. *J Neurochem* 112:24–33
Yudkoff M, Daikhin Y, Nissim I, Horyn O, Lazarow A, Luhovyy B, Wehrli S, Nissim I (2005) Response of brain amino acid metabolism to ketosis. *Neurochem Int* 47:119–28

Supplementary Information accompanies the paper on the Journal of Cerebral Blood Flow & Metabolism website (http://www.nature.com/jcbfm)